2010 3rd International Conference on Computer and Electrical Engineering (ICCEE 2010)
IPCSIT vol. 53 (2012) © (2012) IACSIT Press, Singapore
DOI: 10.7763/IPCSIT.2012.V53.No.2.18

Quadrotor Trajecotry Tracking Control: A PD Control Algorithm

Zongyu Zuo+

The Seventh Research Division, Beihang University (formerly Beijing University of Aeronautics and Astronautics), National Key Laboratory of Science and Technology on Holistic Control

Beijing, China

Abstract—This paper constructs a relationship between attitude and translational movement of a quadrotor, and presents a PD logic tracking control design algorithm capable of not only stabilizing attitude but also tracking a desired trajectory accurately. In contrast to conventional flight control systems, the artificial inner-/outer-loop structure is eliminated via using a third-order time optimal tracking-differentiator. Simulation results demonstrate a better performance than that of conventional ones with timescale separation requirement.

Keywords-PD control; quadrotor; trajectory tracking; tracking-differentiator

1. Introduction

Quadrotor aircraft, consisting of four individual rotors of "X" arrangement, has some advantages over conventional helicopters in view of its configuration. In order to compensate the effect of the reactive torques, the four rotors are divided into two pairs of (1, 3) and (2, 4) turning in opposite direction, as shown in Fig.1. Hence, a quadrotor aircraft is suitable for hover and pseudo-static flight.

The quadrotor is a typical under-actuated, nonlinear coupled system: vertical motion created by collectively increasing and decreasing the speed of all four rotors; pitch or roll motion is achieved by the differential speed of the front-rear set or the left-right set of rotors, coupled with lateral motion; yaw motion is realized by the different reactive torques between the (1, 3) and (2, 4) rotors. And thus the number of individual manipulating variables cannot instantaneously set the accelerations in all directions of the configuration space. In spite of configuring four rotors, the quadrotor is still an under-actuated and nonlinear coupled system.

Pounds [1], McKerrow [2] and Hamel [3] studied the dynamical model of the four-rotor VTOL without considering the aerodynamic effects in their literature. Tayebi *et al* [4] made a slight modification of the gyroscopic torque expression on the dynamical model in [1] and [2], and designed an attitude stabilization PD^2 controller in unit quaternion frame that was frequently employed by spacecaft attitude control problem [5, 6]. Bouabdallah [7] applied the classical PID and LQ algorithm respectively to quadrotor attitude stabilization. However, the under-actuated and strong coupled properties of the quadrotor render the trajectory tracking control design much more challenging. In [8], Bouabdalla achieved the quadrotor trajectory tracking control using backstepping and sliding-mode techniques respectively based on classical inner-/outer-loop structure, but the two-timescale separation assumption requires large inner-loop gain to guarantee closed-loop stability [9]. Madani *et al* [10], [11] divided the quadrotor dynamics into three subsystems and adopted the same methodology to track the desired trajectory via full state backstepping approach. As for the uncertainty and the unknown dynamics, Waslander and Hoffmann [12] designed respectively an integral sliding mode and a

+ Corresponding author.
E-mail address: zzybobby@smss.buaa.edu.cn

reinforcement learning control scheme to make a comparison, and the results demonstrated good robustness of the both controllers.

The motion equations of a rotary aircraft contain translation and rotation of two components, and this classification of the controls as force and moment generating is an artifact of the inner-loop-outer-loop control design strategy [13]. The conventional manipulation when designing control systems for air vehicles is the timescale assumption, which allows the inner loop and outer loop to be designed separately but requires the outer-loop bandwidth to be much slower than that of the inner-loop. This paper first constructs respectively the position and the attitude closed-loop equations employing PD nonlinear feedback linearization technique [14]. To alleviate the timescale problem between attitude and linear dynamics, a time optimal third-order tracking-differentiator is then introduced within the inner-/outer-loop structure. The time optimal third-order tracking-differentiator (TD) proposed in this paper is extended from the second-order TD derived in [15]. This kind of TD can achieve the convergence of non-zero initial state to the origin in three steps, which results in better performance in alleviating the timescale separation than that of classical linear TD. Since the outer-loop bandwidth is closer to that of the inner loop, position tracking performance is increased. Finally, a simulation comparison with a control design algorithm in [16] which requires the timescale separation assumption demonstrates a better performance of the control design presented in this paper.

The paper is organized as follows. Section Ⅱ presents the mathematical model of a quadrotor. Section Ⅲ develops a trajectory tracking control design algorithm, and section Ⅳ is devoted to stability analysis of the closed-loop control system as well as guidelines for parameter selection. In section Ⅴ, numerical simulation of the proposed controller is discussed. Section Ⅵ is the conclusion of this paper.

2. Quadrotor's Nonlinear Model

In view of modeling the quadrotor, several reasonable assumptions are first made: 1) quadrotor is a rigid body; 2) aerodynamics can be ignored at low speed; and 3) quadrotor is symmetrical with respect to axes Ox, Oy and Oz.

Let $\mathcal{I}=\{O_e x_e y_e z_e\}$ denote an earth-fixed inertial frame and $\mathcal{A}=\{Oxyz\}$ a body-fixed frame whose origin O is at the center of mass of the quadrotor, as shown in Fig. 1. The absolute position of the quadrotor is defined by $\boldsymbol{p}=(x,y,z)^T$ and the attitude of the quadrotor by three Euler angles $\boldsymbol{\Theta}=(\phi,\theta,\psi)^T$. $\boldsymbol{R}\in SO(3)$ is the orthogonal rotation matrix to orient the quadrotor.

$$\boldsymbol{R}=\begin{bmatrix} c_\theta c_\psi & s_\theta c_\psi s_\phi - s_\psi c_\phi & s_\theta c_\psi c_\phi + s_\psi s_\phi \\ c_\theta s_\psi & s_\theta s_\psi s_\phi + c_\psi c_\phi & s_\theta s_\psi c_\phi - c_\psi s_\phi \\ -s_\theta & c_\theta s_\phi & c_\theta c_\phi \end{bmatrix}$$

where $s_\theta \triangleq \sin\theta$, $c_\theta \triangleq \cos\theta$ and others are similar. The quadrotor is a six-degree-of-freedom rigid described by three translations $\boldsymbol{v}=(v_x,v_y,v_z)^T$ and three rotations $\boldsymbol{\Omega}=(p,q,r)^T$. The quadrotor motion equations can be therefore expressed as

$$\dot{\boldsymbol{p}}=\boldsymbol{v} \tag{1}$$

$$\dot{\boldsymbol{\Theta}}=\boldsymbol{W}\boldsymbol{\Omega} \tag{2}$$

$$m\dot{\boldsymbol{v}}=-mg\boldsymbol{e}_z+T\boldsymbol{R}\boldsymbol{e}_z \tag{3}$$

$$\boldsymbol{I}_f\dot{\boldsymbol{\Omega}}=-\boldsymbol{\Omega}\times\boldsymbol{I}_f\boldsymbol{\Omega}-\boldsymbol{G}_a+\boldsymbol{\tau}_a \tag{4}$$

where

$$\boldsymbol{W}=\begin{bmatrix} 1 & \sin\phi\tan\theta & \cos\phi\tan\theta \\ 0 & \cos\phi & -\sin\phi \\ 0 & \sin\phi\sec\theta & \cos\phi\sec\theta \end{bmatrix},$$

$\boldsymbol{S}(\boldsymbol{\Omega})$ is a skew-symmetric matrix, m denotes the mass of quadrotor, g the gravity acceleration, $\boldsymbol{e}_z=(0,0,1)^T$ the unit vector, and T the total thrust produced by the four rotors:

$$T=\sum_{i=1}^{4} f_i = b\sum_{i=1}^{4}\omega_i^2 \tag{5}$$

The rotor dynamics are $I_r\dot{\omega}_i=\tau_i-Q_i$, $(i=1,2,3,4)$ where I_r and ω_i denote respectively the moment of inertial and the speed of the rotor i, τ_i is the electrical torque of DC motor, and Q_i is the reactive torque caused by air drag and given by $Q_i = k\omega_i^2$, where the parameters b and k are some positive constants relative to air density and shape of the blade, *et al*. The vector $\boldsymbol{G}_a$ denotes the gyroscopic torque and is given by

$$\boldsymbol{G}_a = \sum_{i=1}^{4} I_r \left(\boldsymbol{\Omega} \times \boldsymbol{z}_e\right)(-1)^{i+1} \omega_i \tag{6}$$

Let l be the distance from the rotors to the center of mass, and then the control torques generated by the four rotors can be calculated as

$$\boldsymbol{\tau}_a = \begin{pmatrix} \tau_a^1 \\ \tau_a^2 \\ \tau_a^3 \end{pmatrix} = \begin{pmatrix} bl\left(\omega_4^2 - \omega_2^2\right) \\ bl\left(\omega_3^2 - \omega_1^2\right) \\ k\left(\omega_2^2 + \omega_4^2 - \omega_1^2 - \omega_3^2\right) \end{pmatrix} \tag{7}$$

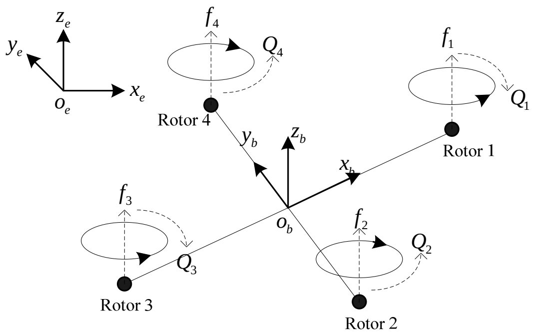

Fig.1. Quadrotor Concept.

3. Control Design Methodology

In consideration of under-actuated and strong coupled properties of a quadrotor, this paper proposes a PD logic design based tracking controller without introducing classical inner-/outer-loop structure, as shown in Fig. 2. A retrofit is performed by employing a complementary third-order time optimal TD to estimate the dynamics of the commanded differential signals quickly instead of ignoring them or computing them tediously. And then compensate the estimated dynamics of the commanded differential signals into the attitude stabilization control law calculation.

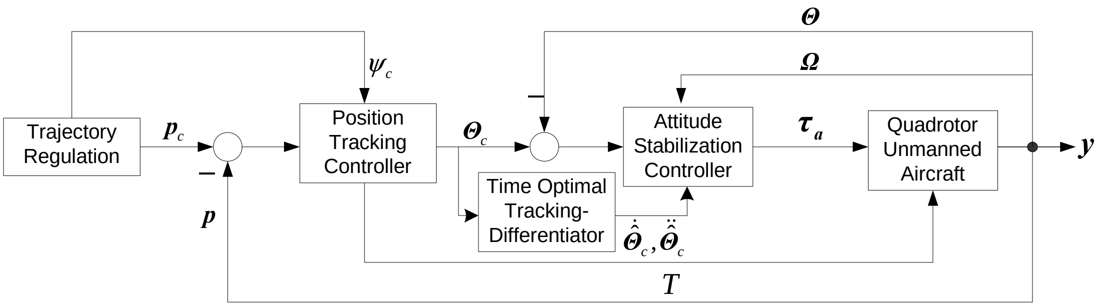

Fig.2. Control Block Diagram

3.1. Position tracking control design

Define the position error

$$\boldsymbol{p}_e \triangleq \boldsymbol{p}_c - \boldsymbol{p}$$

where vector $\boldsymbol{p}_c = \left(x_c, y_c, z_c\right)^T$ is the position commanded value. Then construct the position closed-loop equation as

$$\ddot{\boldsymbol{p}}_e + \boldsymbol{K}_1 \dot{\boldsymbol{p}}_e + \boldsymbol{K}_2 \boldsymbol{p}_e = 0 \tag{8}$$

where $\boldsymbol{K}_1$ and $\boldsymbol{K}_2$ are both positive definite matrix. According to Routh-Hurwitz criterion, position error $\boldsymbol{p}_e$ converges to zero exponentially. Continuously, equation (8) can be rewrite as follows:

$$\ddot{\boldsymbol{p}} = \ddot{\boldsymbol{p}}_c + \boldsymbol{K}_1\left(\dot{\boldsymbol{p}}_c - \dot{\boldsymbol{p}}\right) + \boldsymbol{K}_2\left(\boldsymbol{p}_c - \boldsymbol{p}\right) \tag{9}$$

Define virtual control signal $\boldsymbol{U} \triangleq \ddot{\boldsymbol{p}} = \left(U_1, U_2, U_3\right)^T$ and replace it into (3). We have

$$\boldsymbol{U} = -g\boldsymbol{e}_z + T\boldsymbol{R}\boldsymbol{e}_z / m$$

Moving the gravity acceleration item $-g\boldsymbol{e}_z$ to the left-hand side and then left multiplying rotation matrix $\boldsymbol{R}^T$ on both sides of the preceding equation yields

$$\boldsymbol{R}^T\left(\boldsymbol{U} + g\boldsymbol{e}_z\right) = T\boldsymbol{e}_z / m \tag{10}$$

i.e.

$$\begin{bmatrix} c_\theta c_\psi & c_\theta s_\psi & -s_\theta \\ s_\theta c_\psi s_\phi - s_\psi c_\phi & s_\theta s_\psi s_\phi + c_\psi c_\phi & c_\theta s_\phi \\ s_\theta c_\psi c_\phi + s_\psi s_\phi & s_\theta s_\psi c_\phi - c_\psi s_\phi & c_\theta c_\phi \end{bmatrix} \begin{bmatrix} U_1 \\ U_2 \\ U_3 + g \end{bmatrix} = \frac{1}{m}\begin{bmatrix} 0 \\ 0 \\ T \end{bmatrix}$$

After simple algebraic computation, the following equations hold:

$$U_1 c_\theta c_\psi + U_2 c_\theta s_\psi - \left(U_3 + g\right) s_\theta = 0 \tag{11}$$

$$U_1\left(s_\theta c_\psi s_\phi - s_\psi c_\phi\right) + U_2\left(s_\theta s_\psi s_\phi + c_\psi c_\phi\right) + \left(U_3 + g\right) c_\theta s_\phi = 0 \tag{12}$$

$$U_1\left(s_\theta c_\psi c_\phi + s_\psi s_\phi\right) + U_2\left(s_\theta s_\psi c_\phi - c_\psi s_\phi\right) + \left(U_3 + g\right) c_\theta c_\phi = T / m \tag{13}$$

Using the fact that $\cos\theta$ is non-zero, both sides of (11)can be divided by $\cos\theta$ and pitch expression is obtained:

$$\theta = \arctan\left[\left(U_1\cos\psi + U_2\sin\psi\right) / \left(U_3 + g\right)\right] \tag{14}$$

Equation (13)$\times\sin\phi -$(12)$\times\cos\phi$ yields

$$T\sin\phi / m = U_1\sin\psi - U_2\cos\psi \tag{15}$$

Using (10), the following relationship can be obtained

$$U_1^2 + U_2^2 + \left(U_3 + g\right)^2 = \left(T / m\right)^2 \tag{16}$$

Combining (16) with (15) yields

$$\phi = \arcsin\left[\left(U_1\sin\psi - U_2\cos\psi\right) / \sqrt{U_1^2 + U_2^2 + \left(U_3 + g\right)^2}\right] \tag{17}$$

To this end, equations (14) and (17) can be used to compute the required attitude command inputs to the rotation control design, and the virtual control signal $\boldsymbol{U}$ can be computed from (9). The closed-form expressions for pitch and roll attitudes are

$$\begin{cases} \theta_c = \tan^{-1}\left[\left(U_1\cos\psi + U_2\sin\psi\right) / \left(U_3 + g\right)\right] \\ \phi_c = \sin^{-1}\left[\left(U_1\sin\psi - U_2\cos\psi\right) / \sqrt{U_1^2 + U_2^2 + \left(U_3 + g\right)^2}\right] \end{cases}$$

where ψ_c is commanded yaw attitude. Besides, the total control thrust generated by the four rotors can be computed from (13):

$$T = m[U_1\left(s_\theta c_\psi c_\phi + s_\psi s_\phi\right) + U_2\left(s_\theta s_\psi c_\phi - c_\psi s_\phi\right) + \left(U_3 + g\right) c_\theta c_\phi]$$

3.2. Attitude stabilization control design

Similar to position tracking control design, first construct the attitude error closed-loop equation as

$$\ddot{\boldsymbol{\Theta}}_e + \boldsymbol{K}_3\dot{\boldsymbol{\Theta}}_e + \boldsymbol{K}_4\boldsymbol{\Theta}_e = 0 \tag{18}$$

where vector $\boldsymbol{\Theta}_e \triangleq \boldsymbol{\Theta}_c - \boldsymbol{\Theta}$ denotes the attitude tracking error and $\boldsymbol{\Theta}_c = \left(\phi_c, \theta_c, \psi_c\right)^T$ the commanded attitudes. Gain matrix $\boldsymbol{K}_3$ and $\boldsymbol{K}_4$ are both positive, so the error $\boldsymbol{\Theta}_e$ exponentially converges to zero. Substituting (2) and (4) into (18) yields the control torque:

$$\begin{aligned} \boldsymbol{\tau}_a &= \boldsymbol{\Omega}\times\boldsymbol{I}_f\boldsymbol{\Omega} + \boldsymbol{G}_a - \boldsymbol{I}_f\boldsymbol{W}^{-1}\dot{\boldsymbol{W}}\boldsymbol{\Omega} - \boldsymbol{I}_f\boldsymbol{K}_3\boldsymbol{\Omega} \\ &\quad + \boldsymbol{I}_f\boldsymbol{W}^{-1}\boldsymbol{K}_4\left(\boldsymbol{\Theta}_c - \boldsymbol{\Theta}\right) + \boldsymbol{I}_f\boldsymbol{W}^{-1}\left(\ddot{\boldsymbol{\Theta}}_c + \boldsymbol{K}_3\dot{\boldsymbol{\Theta}}_c\right) \end{aligned} \tag{19}$$

To this end, conventional flight control systems separate the control problem into an inner loop that controls attitude and an outer loop that controls the translational movement. Under two-timescale separation assumption, the dynamics of $\dot{\boldsymbol{\Theta}}_c$ and $\ddot{\boldsymbol{\Theta}}_c$ can be ignored within small enough sampling time, i.e. $\dot{\boldsymbol{\Theta}}_c = \ddot{\boldsymbol{\Theta}}_c = 0$. Then, equation (19) can be further simplified as

$$\boldsymbol{\tau}_a = \boldsymbol{\Omega}\times\boldsymbol{I}_f\boldsymbol{\Omega} + \boldsymbol{G}_a - \boldsymbol{I}_f\boldsymbol{W}^{-1}\dot{\boldsymbol{W}}\boldsymbol{\Omega} - \boldsymbol{I}_f\boldsymbol{K}_3\boldsymbol{\Omega} + \boldsymbol{I}_f\boldsymbol{W}^{-1}\boldsymbol{K}_4\left(\boldsymbol{\Theta}_c - \boldsymbol{\Theta}\right) \tag{20}$$

However, this kind of manipulation requires excellent response of the motors and may result in degradation of the performance when the quadrotor leaves the hovering position. Although the commanded signals $\boldsymbol{\Theta}_c$ is known, it is quite complicated and boring to obtain analytically the dynamics $\dot{\boldsymbol{\Theta}}_c$ and $\ddot{\boldsymbol{\Theta}}_c$. To avoid the intricate calculation and the dependence on timescale separation, a complementary third-order time optimal TD is proposed to estimate the commanded signal dynamics. And the discrete-time form is given by

$$\begin{cases} \boldsymbol{U}(k) = -\left[6\left(\boldsymbol{X}_1(k) - \boldsymbol{\Theta}_c\right) + 12fh\boldsymbol{X}_2(k) + 11f^2h^2\boldsymbol{X}_3(k)\right]/6f^3h^3 \\ \boldsymbol{X}_1(k+1) = \boldsymbol{X}_1(k) + h\boldsymbol{X}_2(k) + h^2\boldsymbol{X}_3(k)/2 + h^3\boldsymbol{U}(k)/6 \\ \boldsymbol{X}_2(k+1) = \boldsymbol{X}_2(k) + h\boldsymbol{X}_3(k) + h^2\boldsymbol{U}(k)/2 \\ \boldsymbol{X}_3(k+1) = \boldsymbol{X}_3(k) + h\boldsymbol{U}(k) \end{cases} \tag{21}$$

where h is the sampling time and adjustable parameter f is called filtering-factor. Then the estimated version of derivatives can be replaced with $\hat{\dot{\boldsymbol{\Theta}}}_c = \boldsymbol{X}_2$ and $\hat{\ddot{\boldsymbol{\Theta}}}_c = \boldsymbol{X}_2$. Hence, the control torque is now modified as

$$\begin{aligned} \boldsymbol{\tau}_a &= \boldsymbol{\Omega} \times \boldsymbol{I}_f \boldsymbol{\Omega} + \boldsymbol{G}_a - \boldsymbol{I}_f \boldsymbol{W}^{-1} \dot{\boldsymbol{W}} \boldsymbol{\Omega} - \boldsymbol{I}_f \boldsymbol{K}_3 \boldsymbol{\Omega} \\ &\quad + \boldsymbol{I}_f \boldsymbol{W}^{-1} \boldsymbol{K}_4 \left(\boldsymbol{\Theta}_c - \boldsymbol{\Theta}\right) + \boldsymbol{I}_f \boldsymbol{W}^{-1} \left(\boldsymbol{X}_3 + \boldsymbol{K}_3 \boldsymbol{X}_2\right) \end{aligned} \tag{22}$$

4. Stability Analysis and Parameter Settings

Closed-loop stability of the proposed control system needs to be verified, because in this control design the commanded signal dynamics is estimated by TD instead of calculating them exactly. Substituting (20) into (18) yields

$$\ddot{\boldsymbol{\Theta}}_e + \boldsymbol{K}_3 \dot{\boldsymbol{\Theta}}_e + \boldsymbol{K}_4 \boldsymbol{\Theta}_e = \ddot{\tilde{\boldsymbol{\Theta}}}_c + \dot{\tilde{\boldsymbol{\Theta}}}_c \tag{23}$$

where $\tilde{\boldsymbol{\Theta}}_e \triangleq \boldsymbol{\Theta}_c - \boldsymbol{X}_1$. The stable tracking error of the attitude is $\boldsymbol{\Theta}_e = \boldsymbol{K}_4^{-1}\left(\ddot{\tilde{\boldsymbol{\Theta}}}_c + \dot{\tilde{\boldsymbol{\Theta}}}_c\right)$. However, the time optimal third-order TD guarantees that the state $\boldsymbol{X}_1$ converges to the commanded input $\boldsymbol{\Theta}_c$ in three steps. Then we have $\tilde{\boldsymbol{\Theta}}_e = \boldsymbol{\Theta}_c - \boldsymbol{X}_1 = 0$ provided $\boldsymbol{\Theta}_c$ keeps constant or slow time-varying within the three steps. In practice this constraint is reasonable since the variation of the position is much slower than the response of TD. Thus, the tracking stable error will converge to zero ultimately, and so is the position tracking error.

Remark: The finite bandwidth of any specified TD or filter results in bounded attitude tracking error. Large parameter $\boldsymbol{K}_4$ can be selected to decrease the ultimate tracking error.

The design parameters of the trajectory tracking controller proposed in this paper include position tracking controller gains $\boldsymbol{K}_1$ and $\boldsymbol{K}_2$, attitude stabilization controller gains $\boldsymbol{K}_3$ and $\boldsymbol{K}_4$, and filtering factor f. The guidelines for the parameter selection are summarized as follows: since the timescale separation requirement between attitude and linear dynamics is alleviated and even eliminated, this control design algorithm only requires each $\boldsymbol{K}_i\ (i = 1,2,3,4)$ to be positive definite. The attitude and the position control gains can be selected independently to satisfy their own bandwidth. Unlike the timescale separation case, larger inner loop gains than outer loop ones have to be satisfied to guarantee the closed-loop stability. The selection of filtering factor f should be a compromise between the control energy and the noise rejection. Besides, too large f will result in more phase-delay of differential signals.

5. Numerical Simulation

In order to verify the effectiveness of the proposed controller, a numerical simulation is performed using data taken from [3], as given in Table 1. Here we will ignore the dynamics of DC motor and only focus on the control law design. The control design parameters in simulation is fixed at $\boldsymbol{K}_1 = \boldsymbol{K}_3 = \mathrm{diag}\{2,2,2\}$, $\boldsymbol{K}_2 = \boldsymbol{K}_4 = \mathrm{diag}\{1,1,1\}$, And the filtering factor is chosen as $f = 10$. In consideration of the limitations of real measuring device, the sampling time is fixed to $h = 0.01\mathrm{sec}$. The initial positions and Euler angles are $\boldsymbol{p}_0 = \boldsymbol{\Theta}_0 = (0,0,0)^T$, so are linear and angular velocities respectively. The desired trajectory is a horizontal rectangle and given by

$$\begin{cases} x_c = t\text{fsg}(t,0,20) + 20\text{fsg}(t,20,40) + (60-t)\text{fsg}(t,40,60) \\ y_c = (t-20)\text{fsg}(t,20,40) + 20\text{fsg}(t,40,60) \\ z_c = 0 \end{cases}$$

where fsg denotes an interval function and is expressed as

$$\text{fsg}(x,a,b) = \left[\text{sign}(x-a) - \text{sign}(x-b)\right]/2$$

where $0 \le a < b$.

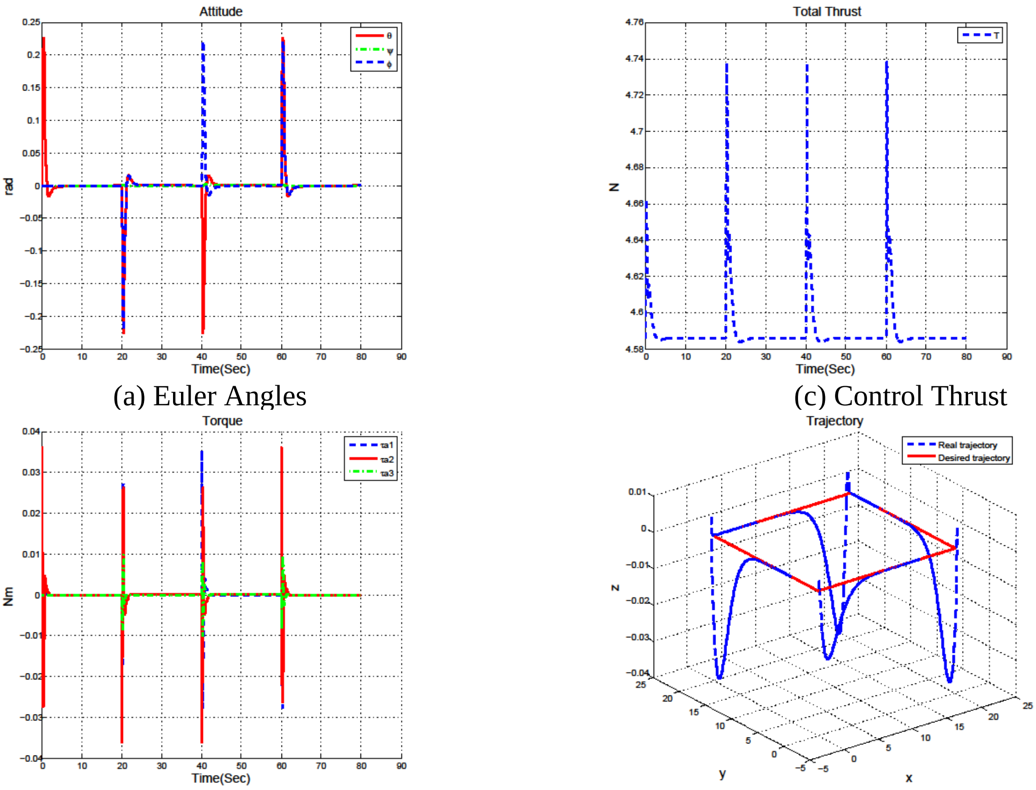

(a) Euler Angles (c) Control Thrust

(b) Control Torque (d) Flight Trajectory

Fig.3. Simulation Result of Horizontal Rectangle Flight

Simulation results is shown in Fig. 3 which depict the time histories of Euler angles, control inputs and flight trajectory. As expected, the design algorithm proposed in this paper make the quadrotor track the desired trajectory in a satisfactory way. By a comparison with the algorithm A in [16] based on the two-timescale separation assumption, the control energy, especially the control torques, as well as trajectory tracking overshoot are much smaller than those of algorithm A. This is due to the result of no longer resorting to the selection of large inner loop gains ($\boldsymbol{K}_3 = 20$ and $\boldsymbol{K}_4 = 100$ in algorithm A) to separate the bandwith between inner and outer loop to guerantee the closed-loop stability. As for the algorithm A, the closed-loop control system is unstable if the same choice of design parameters $\boldsymbol{K}_i\,(i = 1,2,3,4)$ is made as in this section.

TABLE I. QUADROTOR AIRCRAFT MODEL PARAMETERS

Item	**Parameter**				
	$\boldsymbol{m}$	$\boldsymbol{g}$	$\boldsymbol{l}$	$\boldsymbol{I_r}$	$\boldsymbol{I_x}$
Value	0.468	9.81	0.225	3.36×10^{-5}	4.8×10^{-3}
Units	kg	m/s^2	m	kg • m^2	kg • m^2
Item	**Parameter**				
	$\boldsymbol{I_y}$	$\boldsymbol{I_z}$	$\boldsymbol{b}$	$\boldsymbol{k}$	
Value	4.8×10^{-3}	8.8×10^{-3}	2.98×10^{-6}	1.14×10^{-7}	
Units	kg • m^2	kg • m^2	N • s^2/rad^2	N • s2/rad^2	

6. Conclusion

This paper has presented a trajectory tracking control design methodology for a quadrotor unmanned aircraft: a PD control algorithm with a complementary time optimal TD to eliminate two-timescale separation assumption. A main motivation was driven by the requirement of simplifying the computation of commanded derivative signals accurately. In comparison with previous control design algorithm with inner-/outer-loop structure case, the better performance was accomplished by the controller designed in this paper. Finally, numerical simulation of a typical trajectory tracking of a small quadrotor was performed to demonstrate the validity of the proposed controller.

7. Acknowledgment

This work was partially supported by Research Foundation for Key Disciplines of Beijing Municipal commission of Education (XK100060422). The author sincerely acknowledges the motivating discussions with Professor Wei Huo of the Seventh Research Division, Beihang University.

8. References

[1] P. Pounds, R. Mahony, P. Hynes, and J. Roberts, “Design of a Four-Rotor Aerial Robot,” Proc. 2002 Australasian Conf. Robotics and Automation, ARAA Press, Nov. 2002, pp. 145-150.

[2] T. Hamel, R. Mahony, R. Lozano, and J. Ostrowski, “Dynamics Modelling and Configuration Stabilization for an X4-Flyer,” Proc. 15th Triennial World Congress, IFAC Press, 2002, pp. 1-6.

[3] P. McKerrow, “Modeling the Dragonflyer Four-Rotor Helicopter,” Proc. 2004 IEEE International Conf. Robotics and Automation, IEEE Press, Apr. 2004, pp. 3596-3601.

[4] A. Tayebi, and S. McGilvray, “Attitude Stabilization of a Four-Rotor Aerial robot,” Proc. the 43rd IEEE Conf. Decision and Control, IEEE Press, Dec. 2004, pp. 1216-1221

[5] S. M. Joshi, A. G. Kelkar, and J. T. Wen, “Robust Attitude Stabilization of Spacecraft Using Nonlinear Quaternion Feedback,” IEEE Trans. Automatic Control, Vol. 40, 1995, pp. 1800-1803.

[6] F. Lizarrablde, and J. T. Wen, “Attitude Control without Angular Velocity Measurement: A Passivity Approach,” Proc. IEEE International Conf. Robotics and Automation, IEEE Press, 1995, pp. 2701-2706.

[7] S. Bouabdallah, a. Noth, and R. Siegwart, “PID vs LQ Control Techniques Applied to an Indoor Micro Quadrotor,” Proc. 2004 IEEE/RSJ International Conf. Intelligent Robots and Systems, IEEE Press, Sept. 2004, pp. 2451-2456.

[8] S. Bouabdallah, and R. Siegwart, “Backstepping and Sliding-Mode Techniques Applied to an Indoor Micro Quadrotor,” Proc. 2005 IEEE International Conf. Robotics and Automation, IEEE Press, Apr. 2005, pp. 2247-2252.

[9] C. Schumacher, and P. P. Khargonekar, “Stability Analysis of a Missile Control System with a Dynamic Inversion Controller,” J. Guidance, Control, and Dynamics, Vol. 21, 1998, pp. 508-515.

[10] T. Madani, and A. Benallegue, “Control of a Quadrotor Mini-Helicopter via Full State Backstepping Technique,” Proc. 45th IEEE Conf. Decision and Control, IEEE Press, Dec. 2006, pp. 1515-1520.

[11] T. Madani, and A. Benallegue, “Backstepping Sliding Mode Control Applied to a Miniature Quadrotor Flying Robot,” Proc. 32nd Annual Conf. Industrial Electronics (IECON 2006), IEEE Press, Nov. 2006, pp. 700-705.

[12] S. L. Waslander, G. M. Hoffmann, J. S. Jang, and C. J. Tomlin, “Multi-Agent Quadrotor Testbed Control Design: Integral Sliding Mode vs. Reinforcement Learning,” Proc. IEEE/RSJ Conf. Intelligent Robots and Systems (IROS 2005), IEEE Press, Aug. 2005, pp. 3712-3717.

[13] E. N. Johnson, and S. K. Kannan, “Adaptive Trajectory Control for Autonomous Helicopters,” J. Cuidance, Control, and Dynamics, Vol. 28, May-Jun. 2005, pp. 524-538.

[14] J. V. Prasad, R. A. Calise, Y. Pei, and J. E. Corban, “Adaptive Nonlinear Controller Synthesis and Flight Test Evaluation,” Proc. IEEE International Conf. Control Application, IEEE Press, Aug. 1999, pp. 137-142.

[15] Y. Li, “A Complementary Form of the Discrete Tracking-Differentiator,” Proc. International Conf. Measuring Technology and Mechatronics Automation, IEEE Press, Mar. 2010, pp. 46-49.

[16] Z. Zuo, M. Zhu, and Z. Zheng, “Trajectory Tracking Control of a Quadrotor Unmanned Mini-Helicopter,” Proc. 48th AIAA Aerospace Sciences Meeting, AIAA Press, Jan. 2010, pp. 1-13.